Correspondence case report

Drug Testing and Analysis

Received: 9 February 2016 Revised: 15 March 2016 Accepted: 5 April 2016 Published online in Wiley Online Library: 11 May 2016

(www.drugtestinganalysis.com) DOI 10.1002/dta.1986

Detection of LGD-4033 and its metabolites in athlete urine samples

Holly D. Cox* and Daniel Eichner

Introduction

Selective androgen receptor modulators (SARMs) are drugs designed to have tissue-specific activation of the receptor to increase muscle mass and bone density, while avoiding potential negative side effects in other tissues, such as prostate enlargement.[1] This class of drugs is currently under development to treat muscle wasting and bone density loss due to aging, cancer, and chronic illness. The anabolic properties of SARMs make them an attractive potential drug target for athletes wanting to gain an unfair, performance-enhancing advantage and their use is banned by the World Anti-Doping Agency, WADA.[2] LGD-4033 is a nonsteroidal, oral SARM recently developed by Ligand Pharmaceuticals. In clinical trials it was shown to promote a dose-dependent increase in lean body mass after 21 days of treatment, with no significant change in prostate-specific antigen concentrations.[3]

While the drug is not approved for use and is not yet available from the pharmaceutical company, there are several websites claiming to sell the product. The presence of LGD-4033 with the structure 4-(2-(2,2,2-trifluoro-1-hydroxyethyl)pyrrolidin-1-yl)-2-(trifluoromethyl)benzonitrile was confirmed in two products purchased from the Internet in two different laboratories.[4,5] Additionally, the drug was identified in vials confiscated by the German Bureau of Customs Investigation from 2010 to 2013.[6] In the past year, five human samples have been confirmed to contain the drug in the USA, as well as one sample confirmed in Canada. These observations suggest that abuse of the drug may be significant and anti-doping laboratories should include it in their routine screens. Knowledge of the metabolites excreted into urine could further improve the window of detection for LGD-4033.

Thevis *et al*. identified five hydroxylated metabolites of LGD-4033 produced in human liver microsomes.[4] Alternatively, Geldof *et al*. identified five different metabolites produced in human liver microsomes, including hydroxylation with double-bond formation, hydroxylation with pyrrolidine ring cleavage, dihydroxylation, and methoxylation.[5] Using fungal metabolism and electrochemical metabolism simulation, Thevis *et al*. were able to scale-up production of two of the metabolites which allowed structural confirmation by nuclear magnetic resonance (NMR) spectroscopy.[4] While human liver microsomes are frequently used to characterize potential metabolites, the metabolites produced *in vivo* and the relative abundance of each may differ from *in vitro* results. Currently, there are no published studies of LGD-4033 metabolites in human urine samples. In the following report, we describe the metabolites identified in four human urine samples and compared them to the published *in vitro* results. We also identified the metabolites that had the best combination of response and relative abundance that should be included in anti-doping screens to improve the window of detection for the drug.

Experimental

Reagents

LGD-4033 standard with the structure 4-(2-(2,2,2-trifluoro-1-hydroxyethyl)pyrrolidin-1-yl)-2-(trifluoromethyl)benzonitrile was purchased from Cayman Chemical (Ann Arbor, MI, USA). High purity acetonitrile, methanol, methyl tert-butyl ether (MTBE), and formic acid were purchased from VWR International (Radnor, PA, USA). Methyltestosterone was purchased from Steraloids (Newport, RI, USA). Ammonium formate, potassium phosphate, and potassium carbonate were purchased from Sigma-Aldrich (St Louis, MO, USA).

Sample preparation

The urine samples were extracted using a standard protocol for screening banned substances prior to liquid chromatography-tandem mass spectrometry (LC-MS/MS). Briefly, the urine was fortified with internal standard and the pH was adjusted with 200 mM potassium phosphate buffer, pH 7. The samples were treated with β-glucuronidase at 50 °C for 1 h followed by the addition of potassium carbonate buffer, pH 9, and extraction with MTBE. A fraction of the organic layer was collected and evaporated to dryness. The dried samples were resuspended in 33% methanol, 67% 25 mM ammonium formate: 0.1% formic acid in water. Control urine samples included an NQC fortified with internal standard only, a low QC, with anabolic agents fortified at or below the minimum required performance level (MRPL), and a high QC with anabolic agents fortified at twice the concentration of the low QC. The internal standard was methyltestosterone.

LC-MS/MS

Routine screening for banned substances including LGD-4033 was performed by multiple reaction monitoring (MRM) using the Waters Xevo triple quadrupole mass spectrometer coupled to a Waters Acquity I class UPLC system. The analytes were resolved on a Restek Raptor Biphenyl column, (2 x 100 mm, 2.7 μm) at 40 °C with a flow rate of 450 μL/min. Solvent A was 25 mM ammonium formate: 0.1% formic acid in water and Solvent B was acetonitrile. The gradient conditions were 5% to 70% B, 8.5 min; 70% to 95% B, 0.1 min; 95% B, 0.9 min; 95% to 5% B, 0.9 min; and re-equilibration to 5% B for 1.5 min. The instrument was operated in mixed ion mode with a capillary voltage of 2.75 V, cone voltage of 40 V,

* *Correspondence to: Holly D. Cox, Sports Medicine Research and Testing Laboratory, Suite 150A, 560 Arapeen Dr., Salt Lake City, UT 84108, USA. E-mail: hcox@smrtl.org*

Sports Medicine Research and Testing Laboratory, Salt Lake City, UT, 84108

Table 1. Summary of metabolites screened in human urine

Compound	Modification (literature reference)	Proposed Chemical Structure	RT (min)	*Precursor ion (*m/z*)	Collision Energy
LGD-4033	Parent[4,5]	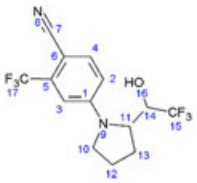	16.39 16.99	337.0776	20
M1	Monohydroxylation of benzonitrile ring[4]	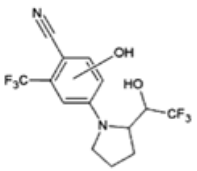	15.52	353.0735	20
M2 A-C	Monohydroxylation of pyrrolidine ring[4]	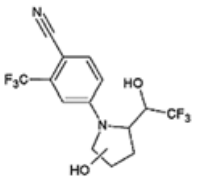	13.33 13.50 13.75	353.0735	20, 40
M3 A-D	Hydroxylation and double bond[5]	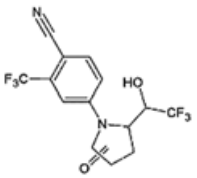	11.67 12.09 12.82 14.27	351.0568	35
M4 A-B	Dihyroxylation of pyrrolidine ring[4,5]	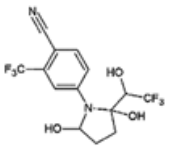	11.66 12.01	369.0674	20, 35
M5	Hydroxylation and pyrrolidine ring cleavage[5,8]	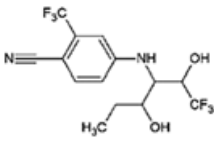	11.91	355.0881	20
M6	Monohydroxylation on both rings[4]	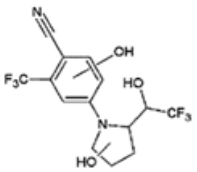	ND	369.0674	35
M7	Methoxylation[5]	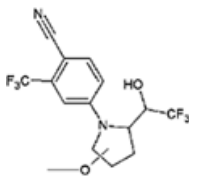	ND	367.0881	35

* Calculated precursor ion *m/z* that was used to generate extracted ion chromatograms.
ND: Not detected

desolvation temperature of 450 °C and nitrogen was used as the collision gas. Two transitions were initially used for screening in positive ion mode: 338.9 > 199, CE = 28 eV and 338.9 > 169.9, CE = 53 eV. After detection, three additional transitions were used for ion ratio confirmation on a different instrument: 339 > 240, 339 > 220, and 339 > 199, CE = 35 eV.

For identification of LGD-4033 metabolites, urine samples were analyzed by high resolution accurate mass spectrometry using the QExactive Plus (ThermoFisher, Waltham, MA, USA) coupled to a Thermo UltiMate 3000 system (ThermoFisher, Waltham, MA, USA). The analytes were resolved using a Waters Acquity BEH C18 column (2.1 x 100 mm, 1.7 μm) at a flow rate of 300 μL/min. Solvent

A was 0.1% formic acid, Solvent B was acetonitrile and the gradient conditions were: 10% to 80% B, 24 min.; hold at 80% B, 0.5 min.; 80% to 10% B, 1.5 min.; and re-equilibration to 10% B for 4 min.

The QExactive Plus was operated using electrospray ionization in negative ion mode with a capillary voltage of -3.75 kV and capillary temperature of 320 °C. Nitrogen gas was used as the collision gas. The instrument was calibrated by external calibration using standards supplied by the manufacturer. Samples were analyzed using full scan mode from *m/z* 100–1000 at a resolution of 35 000 FWHM. Fragmentation of precursor ions of the metabolites was performed using parallel reaction monitoring (PRM) mode at a resolution of 35 000 FWHM with an isolation window of 2.0 Da and a minimum *m/z* 100 set for product ions. Precursor ions and the Normalized Collision Energy (NCE) used are listed in Table 1.

Results

During routine screening of urine samples for anabolic agents, four samples were identified that contained the LGD-4033 parent compound. The presence of the compound was confirmed by comparison of ion ratios for the transitions 339 > 240, 339 > 220, and 339 > 199, to a high QC urine sample spiked with LGD-4033 at 50 ng/mL. The product ion ratios for LGD-4033 in the samples met the criteria for identification as described in the WADA technical document TD2015IDCR.[7] The concentration of LGD-4033 in the urine samples was estimated by comparison of the peak area in the samples to the peak area in the high QC. The concentration detected in the samples was 1700 ng/mL, 900 ng/mL, 200 ng/mL, and 100 ng/mL. The time of administration and the dosing regimen is unknown. After confirmation, the samples were further analyzed to identify metabolites of the drug. The seven metabolites included in the full scan and product ion scan experiments are listed in Table 1. The observed metabolites described below were consistent across the four positive urine samples.

The extracted ion chromatogram for the parent compound in negative ion mode, *m/z* 337.0776, revealed the presence of two peaks which upon fragmentation, had identical product ion spectra. The additional peak for the parent at 16.99 min was present only in the positive urine samples, but not in the NQC or the HQC, which was fortified with the compound (Figure 1). We hypothesize that this additional peak may result from a partial epimerization of the drug *in vivo*. However, other explanations for the additional peak are possible. The presence of the second peak may provide additional qualitative information to confirm the presence of the parent in an unknown sample. The product ion spectra had an abundant ion at *m/z* 267 resulting from the loss of trifluoromethane, *m/z* 70 (Figure 2A). The same preferred site of fragmentation is observed in some of the metabolites and may infer sites of hydroxylation, as discussed below. The abundant product ion at *m/z* 170 results from loss of the pyrrolidine ring, leaving only the trifluoromethylbenzonitrile ring. The presence of this product ion, as well as *m/z* 185, is observed only in metabolites that contain an unmodified benzonitrile ring (Figure 2).

The extracted ion chromatogram for the monohydroxylated metabolites M1 and M2, *m/z* 353.0725, revealed four peaks with different fragmentation behaviour and product ion spectra (Figure 3). The peak at retention time 15.52 min had poor fragmentation at 20 V, but fragmented well at 40 V. The resulting product ions matched those previously described for the metabolite that may be monohydroxylated on the benzonitrile ring (M1) (Figure 2B). This is supported by the presence of the product ion at *m/z* 200,

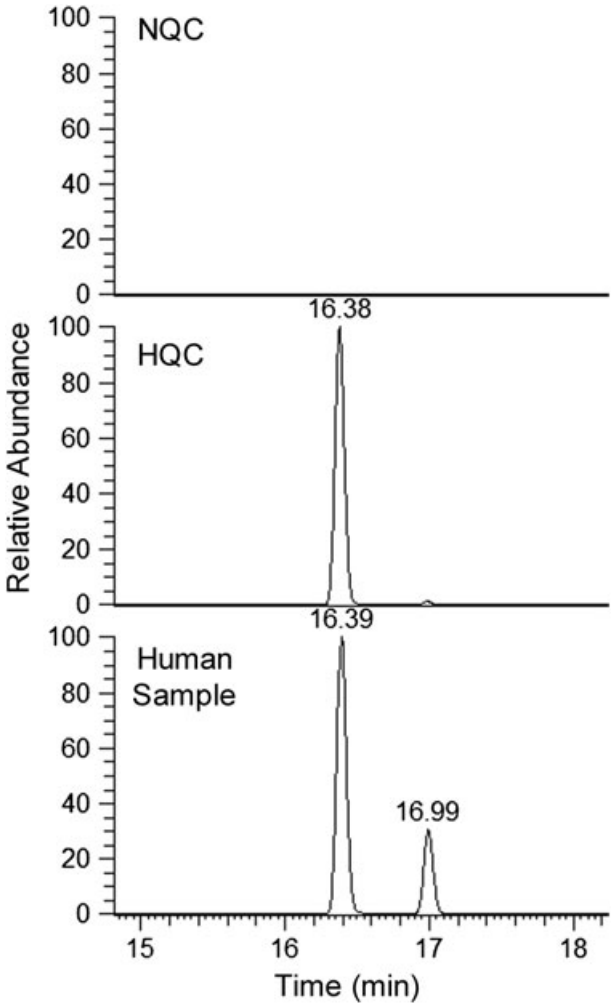

Figure 1. Extracted ion chromatogram of LGD-4033, *m/z* 337.0776, in the NQC, HQC and in a human urine sample.

which represents the hydroxylated form of *m/z* 185 observed in the parent, minus a hydrogen. The same site of fragmentation is suggested (Figure 2B). Likewise, there is an absence of the product ions characteristic of the unmodified benzonitrile ring, *m/z* 170 and 185. These observations support the presence of the M1 metabolite. As was observed for the parent compound, loss of trifluoromethane results in production of the base peak ion, now hydroxylated, at *m/z* 283. Additionally, five product ions were identified with a mass error of less than 5 ppm and the product ion spectra agree well with the published spectra (Table 2). The specific site of hydroxylation on the benzonitrile ring is unclear.

In contrast to the M1 peak at 15.52 min, the peaks at 13.33 min (M2A), 13.50 min (M2B), and 13.75 min (M2C) fragmented well at 20 eV. The product ion spectra also differ from the M1 spectra (Figures 2C and 2D). All three peaks contained product ions corresponding to the unmodified benzonitrile ring, *m/z* 185 and 170. This suggested that the peaks may represent metabolites with a monohydroxylated pyrrolidine ring with hyrdroxylation at different positions. The product ion spectra for the peak at 13.50 min (M2B) had a base peak ion at *m/z* 227 rather than *m/z* 283, suggesting that hydroxylation on the pyrrolidine ring promotes further fragmentation of the ring. The spectra of the M2B metabolite, shown in Figure 2D, closely match that of the metabolite previously identified in human liver microsomes in which the site of hydroxylation

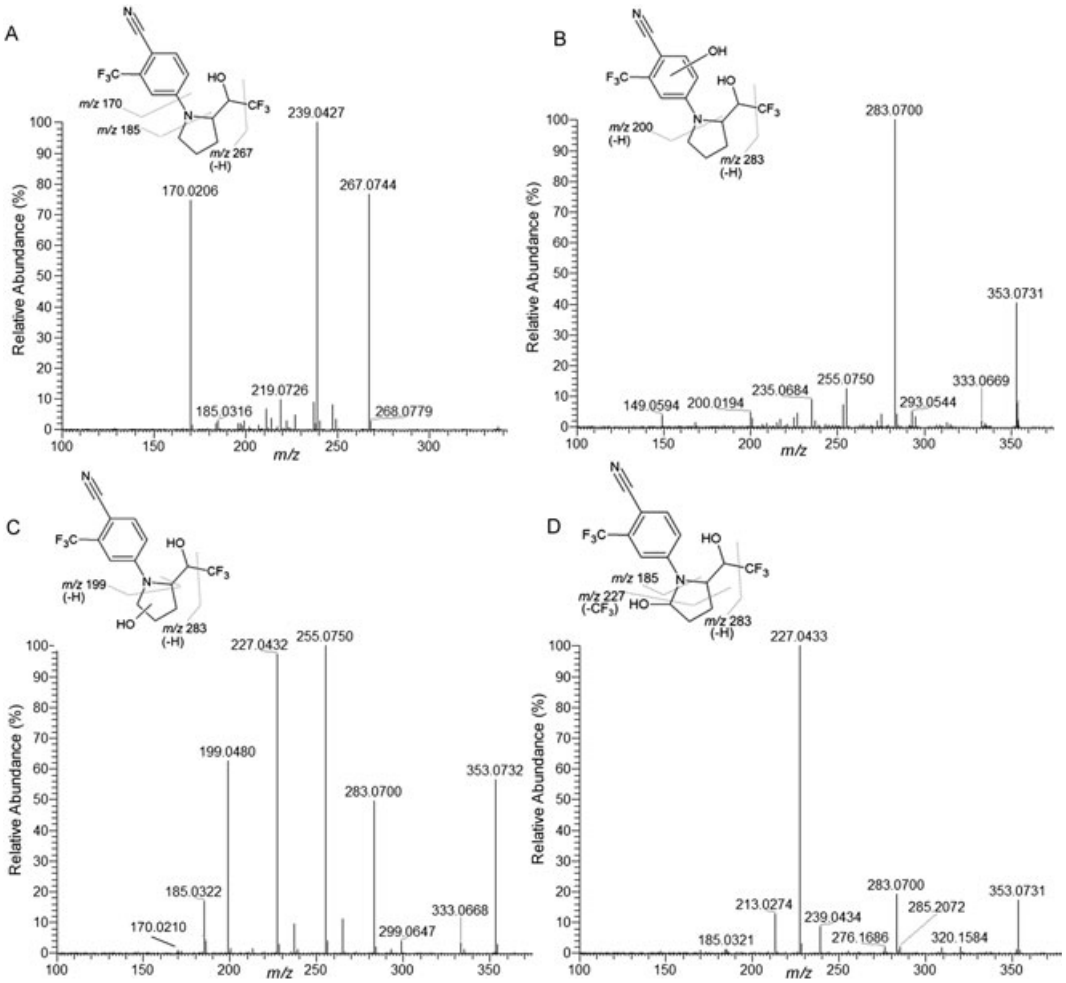

Figure 2. Product ion spectra for the parent (A), M1 metabolite (B), M2A/C metabolite (C) and M2B metabolite (D) observed in negative ion mode. Structures are [M-H]-.

was confirmed by NMR. For the *in vitro* metabolite, hydroxylation was closest to the pyrrolidine nitrogen at C-10. Six product ions were identified for this metabolite with an error of less than 5 ppm (Table 2). In contrast, the product ion spectra for the M2A and M2C metabolites differ significantly from the M2B metabolite and have not been previously reported in human liver microsomes (Figure 2C). Both spectra contain product ions at *m/z* 255 and 199 with a high relative abundance to the base peak at *m/z* 227. The product ion at *m/z* 255 may result from the loss of the trifluoromethane, to produce *m/z* 283, followed by loss of carbon monoxide. The difference in the three spectra suggests that fragmentation of the pyrrolidine ring is dependent upon the site of hydroxylation, and hydroxylation closer to the trifluorohydroxyethyl group may promote additional fragmentation to form *m/z* 199 and 255. Additionally, preferred sites of monohydroxylation in the human urine samples appear to differ from that observed in human liver microsomes where M2B was the primary metabolite. Given the poor chromatography and multiple sites of modification for the monohydroxylated pyrrolidine metabolites, it would be difficult to implement them into anti-doping screens for LGD-4033.

While Thevis *et al.* reported the formation of monohydroxylated metabolites in human liver microsomes, Geldof *et al.* reported the presence of a metabolite containing a hydroxylation and a double bond, or possibly a carbonyl, on the pyrrolidine ring rather than hydroxylation, shown as M3 in Table 1.[4,5] The extracted ion chromatogram for M3 metabolites at *m/z* 351.0568 showed five peaks identified in human urine possibly representing multiple sites for the modification (Figure 3). Upon fragmentation, the product ion spectra for each peak was identical, but was different from that obtained for the monohydroxylated metabolites discussed above, M1 and M2. The presence of the product ions at *m/z* 170 and 185 representing the unmodified benzonitrile ring, suggest that the modification occurs on the pyrrolidine ring. It should be noted that the retention time for two metabolites at *m/z* 351 at 11.67 min and 12.01 min match the retention time for the two dihydroxylated metabolites at *m/z* 369. Additionally, the metabolites at *m/z* 369 readily lose H_2O upon fragmentation to produce *m/z* 351 in the product ion spectra (Figure 4). Therefore, it is possible that at least two of the metabolites observed at *m/z* 351 may result from in-source fragmentation and concomitant loss of H_2O by the dihydroxylated metabolites at *m/z* 369. As discussed below and shown in Table 3, the relative abundance of the dihydroxylated metabolite at *m/z* 369 is approximately 50-fold greater than the metabolite at *m/z* 351 at 11.67 min, further supporting the idea that a small fraction of *m/z* 369 is lost to in-source fragmentation. It is unclear if the three additional peaks for the *m/z* 351 metabolite at 12.09 min, 12.82 min and 14.27 min are the result of in-source fragmentation or are true metabolites, since no matching peaks were identified for the *m/z* 369 metabolite. Previous work reported by Geldof *et al.* showed a different retention time for the *m/z* 351 and *m/z* 369 metabolites,

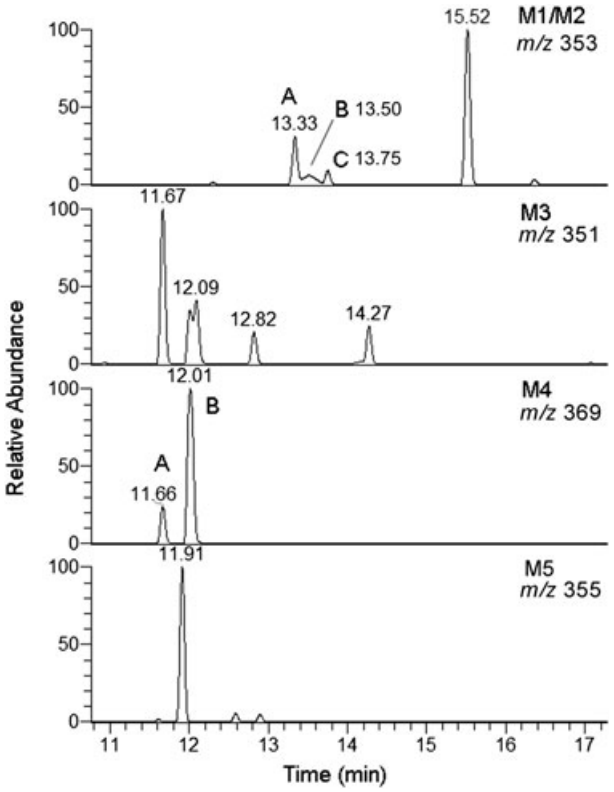

Figure 3. Extracted ion chromatogram of the metabolites of LGD-4033 detected in human urine.

suggesting that *m/z* 351 can be a true metabolite *in vitro*.[5] Five product ions match those previously reported for the metabolite with an error of less than 7 ppm (Table 2).

Both previous *in vitro* reports have identified a dihydroxylated metabolite with both modifications on the pyrrolidine ring. In human urine samples, the extracted ion chromatogram for *m/z* 369.0674 showed two peaks (Figure 3). The product ion spectra for the two peaks are the same with the exception of the relative abundance of *m/z* 253 and 255 (Figure 4). In M4A at 11.66 min, *m/z* 253 is significantly greater than *m/z* 255, while in M4B at 12.01 min, *m/z* 253 and 255 are of nearly equal abundance. Additionally, the product ion spectra for the dihydroxylated metabolites is the same as the product ion spectra for the M3A and M3B metabolites containing a single hydroxylation and double bond at *m/z* 351. Thus it is possible that upon fragmentation, the dihydroxylated metabolite readily loses H_2O to form the M3 metabolite, *m/z* 351, and fragmentation then proceeds by the same pathway. Ten product ions were identified that match those previously reported with an error of less than 6 ppm (Table 2). The structure of the dihydroxylated metabolite reported by Thevis *et al*. was confirmed by NMR analysis to demonstrate that hydroxylation occurs on position C-10 and C-11 (Table 1).[4] The product ion spectra they reported matched well with the M4B metabolite in our work with *m/z* 255 at a higher relative abundance. Additionally, when the collision energy was adjusted to NCE of 20 V, as was used in the previous report, then the base ion peak and relative abundance of the product ions matched well (data not shown).[4] Therefore, it is likely that the structure of the M4B metabolite has the same structure described previously and confirmed by NMR.

Table 2. Proposed elemental composition of the observed product ions for LGD-4033 and the metabolites in negative ion mode

Compound	Precursor Ion (m/z)	Chemical Formula	Error (ppm)	Product Ion (m/z)	Chemical Formula	Error (ppm)	Cleaved Species
LGD-4033	337.0781	$C_{14}H_{11}ON_2F_6$	1.60	267.0744	$C_{13}H_{10}ON_2F_3$	−0.45	-HCF_3
				239.0427	$C_{11}H_6ON_2F_3$	−2.09	-HCF_3
							-C_2H_4
				211.0475	$C_{10}H_6N_2F_3$	−3.79	-HCF_3
							-C_2H_4
							-CO
				185.0316	$C_8H_4N_2F_3$	−5.94	-$C_6H_7OF_3$
				170.0206	$C_8H_3NF_3$	−6.47	-HCF_3
							-C_2H_4
							-C_3H_3NO
M1	353.0733	$C_{14}H_{11}O_2N_2F_6$	2.35	333.0669	$C_{14}H_{10}O_2N_2F_5$	2.10	-HF
				283.0700	$C_{13}H_{10}O_2N_2F_3$	2.12	-HCF_3
				255.0750	$C_{12}H_{10}ON_2F_3$	1.96	-HCF_3, -CO
				235.0684	$C_{12}H_9ON_2F_2$	0.43	-HCF_3, -CO
							-HF
				200.0194	$C_8H_3ON_2F_3$	−1.50	-$C_6H_8OF_3$
M2 A/C	353.0732	$C_{14}H_{11}O_2N_2F_6$	2.07	333.0668	$C_{14}H_{10}O_2N_2F_5$	1.80	-HF
				283.0700	$C_{13}H_{10}O_2N_2F_3$	2.12	-HCF_3
				255.0750	$C_{12}H_{10}ON_2F_3$	1.96	-HCF_3, -CO
				237.0641	$C_{12}H_8N_2F_3$	0.84	-HCF_3, -CO
							-H_2O
				227.0433	$C_{10}H_6ON_2F_3$	0.34	-HCF_3
							- C_3H_4O
				199.0480	$C_9H_6N_2F_3$	−1.51	-$C_5H_5O_2F_3$

(Continues)

Table 2. Continued

Compound	Precursor Ion (m/z)	Chemical Formula	Error (ppm)	Product Ion (m/z)	Chemical Formula	Error (ppm)	Cleaved Species
				185.0322	$C_8H_4N_2F_3$	−1.50	$-C_6H_7O_2F_3$
				170.0210	$C_8H_3NF_3$	−4.12	$-HCF_3$
							$-C_2H_4$
							$-C_3H_3NO$
M2 B	353.0731	$C_{14}H_{11}O_2N_2F_6$	1.78	283.0700	$C_{13}H_{10}O_2N_2F_3$	1.99	$-HCF_3$
				239.0434	$C_{11}H_3ON_2F_3$	0.74	$-HCF_3$
							$-C_2H_4O$
				227.0433	$C_{10}H_6ON_2F_3$	0.34	$-HCF_3$
							$-C_3H_4O$
				213.0275	$C_9H_4ON_2F_3$	−0.34	$-HCF_3$
							$-C_4H_4O$
				185.0321	$C_8H_4N_2F_3$	−3.24	$-C_6H_7O_2F_3$
				170.0210	$C_8H_3NF_3$	−4.12	$-HCF_3$
							$-C_2H_4$
							$-C_3H_3NO$
M3	351.0574	$C_{14}H_9O_2N_2F_6$	1.65	281.0535	$C_{13}H_8O_2N_2F_3$	−1.07	$-HCF_3$
				263.0431	$C_{13}H_6ON_2F_3$	−0.38	$-HCF_3$
							$-H_2O$
				253.0227	$C_{11}H_4O_2N_2F_3$	0.79	$-HCF_3$
							$-C_2H_4$
				237.0634	$C_{12}H_8N_2F_3$	−2.11	$-HCF_3$
							$-CO_2$
				170.0206	$C_8H_3NF_3$	−6.47	$-C_6H_6O_2NF_3$
M4	369.0679	$C_{14}H_{11}O_3N_2F_6$	1.39	351.0566	$C_{14}H_9O_2N_2F_6$	−0.57	$-H_2O$
				299.0647	$C_{13}H_{10}O_3N_2F_3$	1.00	$-HCF_3$
				281.0537	$C_{13}H_8O_3N_2F_3$	−0.36	$-H_2O$, $-HCF_3$
				263.0432	$C_{13}H_6ON_2F_3$	0.00	$-2H_2O$,
							$-HCF_3$
				255.0743	$C_{12}H_{10}ON_2F_3$	−0.78	$-HCF_3$, $-CO_2$
				253.0587	$C_{12}H_8ON_2F_3$	−0.40	$-CHOHCF_3$
							$-H_2O$
				253.0224	$C_{11}H_4O_2N_2F_3$	−0.68	$-HCF_3$, $-C_2H_4$
							$-H_2O$
				237.0636	$C_{12}H_8N_2F_3$	−1.27	$-CO_2$, $-HCF_3$
							$-H_2O$
				185.0317	$C_8H_4N_2F_3$	−5.40	$-C_6H_7O_2F_3$
				170.0207	$C_8H_3NF_3$	−5.88	$-C_6H_8O_3NF_3$
M5	355.0888	$C_{14}H_{13}O_2N_2F_6$	1.91	285.0848	$C_{13}H_{12}O_2N_2F_3$	−1.01	$-HCF_3$
				257.0899	$C_{12}H_{12}ON_2F_3$	−1.05	$-HCF_3$, $-CO$
				239.0790	$C_{12}H_{10}N_2F_3$	−2.54	$-HCF_3$, $-CO$
							$-H_2O$
				237.0634	$C_{12}H_8N_2F_3$	−2.11	$-HCF_3$
							$-CHOH$
							$-H_2O$
				226.0347	$C_{10}H_5ON_2F_3$	−3.08	$-CH_3CH_2CH-OH$
							$-HCF_3$
				199.0473	$C_9H_6N_2F_3$	−5.02	$-C_5H_7O_2F_3$
				185.0315	$C_8H_4N_2F_3$	−6.49	$-C_6H_9O_2F_3$
				170.0206	$C_8H_3NF_3$	−6.47	$-C_6H_{10}O_2NF_3$

Geldof *et al.* reported the presence of a metabolite containing a single hydroxylation on the pyrrolidine ring followed by cleavage of the ring.[5] The extracted ion chromatogram of the human urine samples showed one peak for *m/z* 355.0881 (Figure 3). After fragmentation, eight product ions were identified that matched those reported by Geldof *et al.* with an error of less than 7 ppm (Table 2).[5] While the structure proposed by Geldof *et al.* is shown in Table 1, we suggest that other structures for this metabolite may be more likely to occur. We suggest that ring-opening is more likely to occur at the site of hydroxylation and when hydroxylation occurs at the carbon next to the pyrrolidine nitrogen. Ring-opening could then occur by oxidative dealkylation. Given the product ions observed, it is not possible to determine the site of hydroxylation or the structure of the ring-opened metabolite.

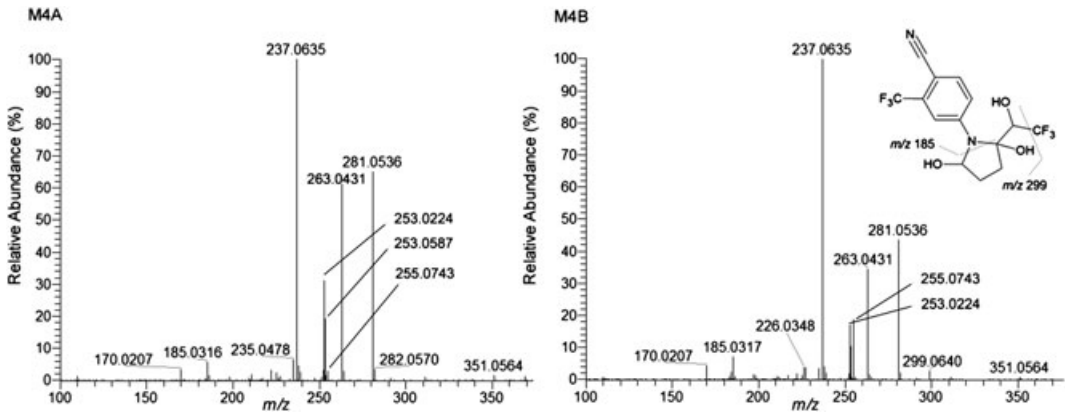

Figure 4. Product ion spectra for the M4A and M4B metabolites in negative ion mode. Structure is [M-H]-.

However, based on the presence of the product ions *m/z* 185 and *m/z* 170, it is clear that the hydroxylation must occur on the pyrrolidine ring.

Thevis *et al*. also reported the presence of a dihydroxylated metabolite with one hydroxylation on each ring also at *m/z* 369.0674.[4] While two peaks were identified for this mass as already discussed, the product ions did not match those previously reported for this metabolite. Geldof *et al*. reported the presence of a metabolite containing a single methoxylation on the pyrrolidine ring with *m/z* 367.0881.[5] However, the extracted ion chromatogram and the product ion scan of human urine samples did not detect a metabolite with that m/z. Therefore, some metabolites produced *in vitro* by human liver microsomes were not observed *in vivo*.

Inclusion of LGD-4033 metabolites in anti-doping screens may improve detection of abuse; however, it is not feasible to include all of the metabolites described and many metabolites have poorly characterized structures. Additionally, it is most valuable to know the relative abundance of the metabolites and which metabolites may persist after loss of the parent thus extending the detection window for the drug. While we cannot determine the true concentration of the metabolites without standards, we measured the peak area of each metabolite relative to the parent in full scan analysis of the human urine samples shown in Table 3. As shown in Table 3, the metabolite/parent ratio was significantly larger for the dihydroxylated metabolite, than for the other metabolites with an average ratio of 55.9 and a range from 48.7 to 64.1 across the four samples. The M5 metabolite with hydroxylation and pyrrolidine ring cleavage was the second most abundant metabolite with an average ratio of 20.7. The other metabolites were significantly lower with average ratios from 1.3 to 2.0. This differs from the *in vitro* observations by Thevis *et al*. where the data suggest that the monohydroxylated pyrrolidine ring metabolite (M2B) was the most abundant and was produced by human liver microsomes, fungal processing methods, and electrochemical conversion methods.[4] Our results are supported by *in vivo* preliminary data which demonstrated that the dihydroxylated metabolite was detectable for up to 190 h post-administration in a single human subject.[8] The same study demonstrated that the parent was detectable at 22 h, but not 190 h, indicating that measurement of the dihydroxylated metabolite may extend the window of detection for some samples. Since the dihydroxylated metabolite appears to have the best response and/or relative abundance in human samples, it should be included in anti-doping screens along with parent compound.

Table 3. Response of each metabolite relative to the parent in human urine

Compound	Average Ratio (metabolite/parent)	Ratio Range (n = 4 samples)
Parent Peak 2	0.56	0.3 – 0.9
M1	1.9	1.1 – 3.6
M2	2.0	1.3 – 2.5
M3	1.3	0.9 – 1.6
M4	55.9	48.7 – 64.1
M5	20.7	11.1 – 34.1
M6	ND	ND
M7	ND	ND

ND: Not detected

Discussion

In summary, we have characterized the metabolites of LGD-4033 identified in four human urine samples and compared them to that previously identified from *in vitro* experiments in human liver microsomes. Unique metabolites characterized in each laboratory were identified in human urine with some differences. The position of monohydroxylation on the pyrrolidine ring appears to differ from the *in vitro* experiments. Additionally, pyrrolidine ring hydroxylation with double bond, M3, appears to have occurred at up to three sites *in vivo*, while only one position was previously reported *in vitro*. Two additional peaks for the M3 metabolite may result from in-source fragmentation. Two metabolites identified *in vitro*, one with hydroxylation on both rings (M6) and one with methoxylation (M7) were not identified *in vivo* using the described methods. The poor chromatography of the M2 A-C metabolites prevents their use in anti-doping screens. In contrast to the *in vitro* data, the dihydroxylated metabolite (M4), had a significantly higher response and/or relative abundance than the other metabolites and may improve detection of the drug in anti-doping laboratories. Further, we demonstrate that LGD-4033 and the hydroxylated metabolites are easily detected using a common method of extraction performed in most anti-doping laboratories.

Acknowledgments

We would like to thank Dr Ryan Van Wagoner at the Sports Medicine Research and Testing Laboratory and Dr James E. Cox in the Department of Biochemistry at the University of Utah for their helpful discussions.

References

[1] S. Bhasin, R. Jasuja. Selective androgen receptor modulators as function promoting therapies. *Curr. Opin. Clin. Nutr. Metab. Care.* **2009**, *12*, 232.

[2] WADA. *Vol. 2016*, The 2016 Prohibited List, International Standard. WADA, Montreal, **2016**. Available at https://wada-main-prod.s3.amazonaws.com/resources/files/wada-2016-prohibited-list-en.pdf (January 2016).

[3] S. Basaria, L. Collins, E. L. Dillon, K. Orwoll, T. W. Storer, R. Miciek, J. Ulloor, A. Zhang, R. Eder, H. Zientek, G. Gordon, S. Kazmi, M. Sheffield-Moore, S. Bhasin. The safety, pharmacokinetics, and effects of LGD-4033, a novel nonsteroidal oral, selective androgen receptor modulator, in healthy young men. *J. Gerontol. A Biol. Sci. Med. Sci.* **2013**, *68*, 87.

[4] M. Thevis, A. Lagojda, D. Kuehne, A. Thomas, J. Dib, A. Hansson, M. Hedeland, U. Bondesson, T. Wigger, U. Karst, W. Schanzer. Characterization of a non-approved selective androgen receptor modulator drug candidate sold via the Internet and identification of in vitro generated phase-I metabolites for human sports drug testing. *Rapid Commun. Mass Spectrom.* **2015**, *29*, 991.

[5] L. Geldof, O. J. Pozo, L. Lootens, W. Morthier, P. Van Eenoo, K. Deventer. In vitro metabolism study of a black market product containing SARM LGD-4033. *Drug Test. Anal.* **2016**.

[6] O. Krug, A. Thomas, K. Walpurgis, T. Piper, G. Sigmund, W. Schanzer, T. Laussmann, M. Thevis. Identification of black market products and potential doping agents in Germany 2010-2013. *Eur. J. Clin. Pharmacol.* **2014**, *70*, 1303.

[7] WADA. WADA Technical Document - TD2015IDCR: Minimum criteria for chromatographic-mass spectrometric confirmation of the identity of analytes for doping control purposes, *Vol. 2016*, 2015 ed., WADA, Montreal, **2015**. Available at https://wada-main-prod.s3.amazonaws.com/resources/files/wada_td2015idcr_minimum_criteria_chromato-mass_spectro_conf_en.pdf (January 2016).

[8] T. Sobolevsky, M. Dikunets, G. Dudko, G. Rodchenkov. Metabolism study of selective androgen receptor modulator LDG-4033. *Manfred Donike Workshop - 33rd Cologne Workshop on Dope Analysis* 1- 6 March **2015**.